

Electronic Properties of Alkali- and Alkaline-Earth-Intercalated Silicon Nanowires

S. Sirichantopass, V. M. García-Suárez, and C. J. Lambert

Department of Physics, Lancaster University, Lancaster, LA1 4YB, U. K.

(Dated: December 2, 2024)

We present a first-principles study of the electronic properties of silicon clathrate nanowires intercalated with various types of alkali or alkaline-earth atoms. We find that the band structure of the nanowires can be tuned by varying the impurity atom within the nanowire. The electronic character of the resulting systems can vary from metallic to semiconducting with direct band gaps. These properties make the nanowires specially suitable for electrical and optoelectronic applications.

PACS numbers: 73.22.-f, 73.21.Hb, 81.07.Vb

The desire for nanoscale components which integrate gracefully with silicon CMOS technology makes the fabrication and characterization of silicon nanowires particularly attractive. These structures can be grown using a broad range of experimental techniques [1, 2, 3, 4, 5, 6] and possess novel properties, which may make them suitable as interconnects in very-large-scale integrated devices. Other interesting applications include photoelectronics, since these structures have large direct band-gaps, which allow them to work as visible-light emitters with low power consumption. The origin of this change in the band gap is related to quantum confinement [7, 14] which increases the band width and produces an indirect-direct transition as the size of the wire shrinks [9]. The band gap generates a low-voltage gap in the I-V characteristic which is considerably enhanced when the surface is passivated [8]. However, upon doping the gap disappears and the resulting I-V curves display ohmic behavior for low voltages [10].

Many possible structures for silicon nanowires have been proposed [3, 8, 9, 11, 12, 13, 14, 15, 16, 17, 18]. Those grown from porous silicon are the most stable for diameters down to 1 nm [9, 17, 18]. However, for smaller diameters, nanowires derived from the silicon clathrate phases are predicted to be the most stable [3, 17]. These nanowires can have many different shapes [8, 9, 17, 18] depending on the basic repeat unit and growth direction.

Clathrates are particularly interesting due to their novel elastic [19], thermoelectric [20], optoelectronic [21] and superconducting [22] properties. They are grown by nucleating a vapor of silicon or other group IV elements such as Ge and Sn around alkali or alkaline-earth atoms generally from the third or larger rows [23]. The impurities can be left inside the structure with different concentrations or be removed afterwards. Pristine clathrates are semiconducting and have wider band gaps than the diamond phase of silicon [24], whereas intercalated clathrates are usually metallic [25]. The most common clathrate lattices have 34 and 46 atoms in the primitive unit cell and are made of Si_{20} and Si_{28} cages and Si_{20} and Si_{24} cages, respectively.

The smallest of the clathrate-type nanowires are based on the Si_{20} and Si_{24} cages [3, 8]. The Si_{20} cage, which is present in both types of bulk clathrates, is a regular polyhedron made of 12 pentagons. The corresponding nanowire is grown along an axis that passes through two opposite faces (C_{5v} symmetry) and has 30 atoms in the unit cell. The Si_{24} cage has 12 pentagons and two opposite hexagons. The corresponding nanowire is grown along the direction perpendicular to the hexagons (C_{6v} symmetry) and contains 36 atoms in the unit cell. The transport properties of this nanowire placed between aluminium electrodes and passivated with hydrogen were calculated by Landman et al. [26], and it was found that the nanowire doped with Al atoms was more efficient than the pristine one. We label these nanowires as Si(30) and Si(36) respectively. The intercalation of alkali or alkaline-earth impurities is made possible by the large endohedral space available inside the cages and the fact that the corresponding bulk structures are stable.

In this article we report ab-initio theoretical studies of the electronic properties of Si(30) and Si(36) nanowires intercalated with the alkali and alkaline-earth metals $\{\text{Na}, \text{K}, \text{Rb}, \text{Cs}\}$ and $\{\text{Ca}, \text{Sr}, \text{Ba}\}$, respectively, which correspond to typical clathrate intercalations [23]. We label them as $2\text{M}@\text{Si}(30)$ and $2\text{M}@\text{Si}(36)$, where 2M represents the two alkali or alkaline earth atoms included in the unit cell. An example of the top and lateral view of these structures is shown in Fig. (1). We predict that intercalation dramatically alters the electronic structure of the nanowires and allows one to tune their electronic properties. These changes arise from a combination of structural deformation, hybridization and charge transfer from

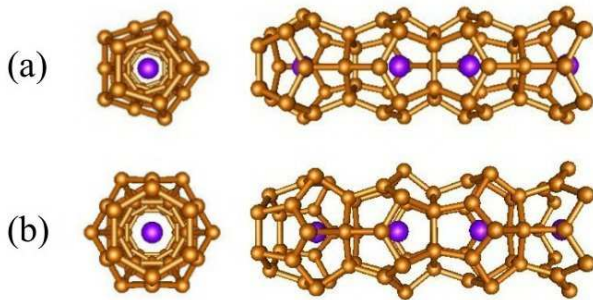


FIG. 1: Top and lateral views of two unit cells of a $2\text{M}@\text{Si}(30)$ (a) and a $2\text{M}@\text{Si}(36)$ (b), where M is an alkali or alkaline-earth atom.

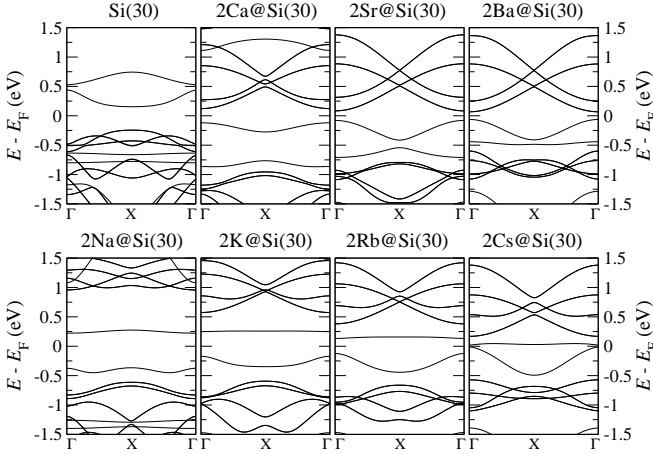


FIG. 2: Band structure of pristine (first top box), alkaline-earth intercalated (next three top boxes) and alkali intercalated (bottom) Si(30) nanowires.

the endohedral impurity. As a consequence, the electronic character of the nanowires can range from metallic to semiconducting. The band gaps in the latter are usually direct and comparable to the band gap of bulk silicon, which make these nanowires particularly useful for optoelectronics applications in the infrared or visible range.

We use the SIESTA code [27], which is based on density functional theory [28] and employs norm-conserving pseudopotentials and linear combinations of atomic orbitals. The valence states are spanned with optimized double- ζ polarized basis sets. In the heaviest atoms (K,Ca,Rb,Sr,Cs,Ba) we include relativistic corrections in the pseudopotentials and semi-core states in the basis set. The exchange and correlation energy and potential are evaluated using the local density approximation (LDA). All atomic coordinates and the lattice are fully relaxed until all the forces and the stress are smaller than 0.02 eV/Å and 1.0 GPa, respectively. The dimensions of the unit cell along the perpendicular directions are chosen large enough to avoid overlaps and electrostatic interactions with other images. The real space grid is defined with a plane wave cutoff of 200 Ry. The Brillouin zone along the nanowire growth direction is sampled with 30 k -points to perform the structural relaxations and with 200 k -points to calculate the densities of states (DOS), where a broadening parameter of 0.01 eV is used. The binding energies are computed by removing the basis set superposition error [29] which comes from the localized character of the basis functions.

First we focus on the pristine nanowires, whose initial unrelaxed configuration corresponds to that of the ideal polyhedral structures. Upon full relaxation the structure changes slightly and compresses, resulting in lattice constants along the growth direction of 10.50 Å and 10.28 Å for the Si(30) and Si(36) wires, respectively. The cohesive energies of both nanowires are very similar, as can be seen in Table I. The Si(36) is slightly more stable [3], which is probably due to the fact that in this nanowire the presence of sixfold rings generates bond

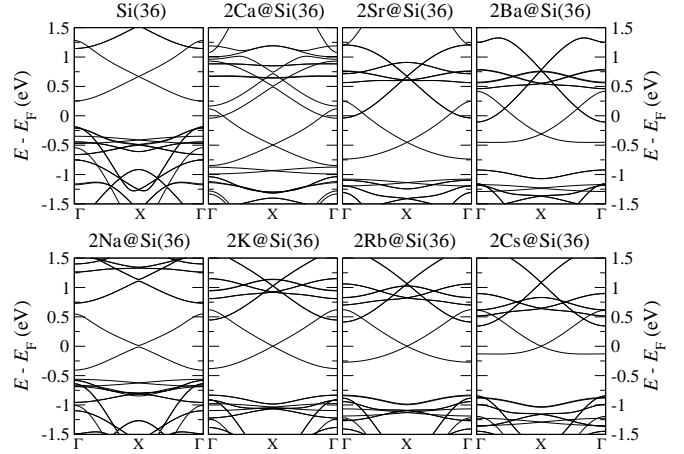


FIG. 3: Band structure of pristine (first top box), alkaline-earth intercalated (next three top boxes) and alkali intercalated (bottom) Si(36) nanowires.

TABLE I: Binding energies (BE) and band gaps (BG) of pristine and alkali- or alkaline-earth intercalated Si(30) and Si(36) nanowires.

	Si(30)		Si(36)	
	BE (eV)	BG (eV)	BE (eV)	BG (eV)
Pristine	-5.22	0.40	-5.25	0.44
Na	-2.25	0.60	-2.42	0.03
K	-1.40	0.42	-2.47	0.00
Rb	-0.72	0.26	-2.37	0.00
Cs	0.42	0.03	-2.08	0.00
Ca	-3.70	0.24	-4.88	0.00
Sr	-3.86	0.16	-4.52	0.00
Ba	-4.33	0.13	-5.67	0.00

angles much closer to the ideal bond angles of diamond silicon and reduces the strain of the structure. The electronic band structures computed for the pristine Si(30) and Si(36) nanowires are shown in the first boxes of Figs. (2) and (3), respectively. The Si(30) nanowire has a direct band gap at the X point with a LDA value of 0.40 eV. Taking into account that the LDA underestimates bands gaps, but gives correct relative orders and trends, this would imply, after a scissor-correction of 0.7 eV, which is usually employed in silicon [24], a true band gap of \sim 1.10 eV, similar to the band gap of diamond silicon. The Si(36) nanowire also has a direct band gap of 0.44 eV but it is located at the Γ instead of the X point. The scissor correction gives in this case a value of 1.14 eV. The character and width of such band gaps, which lie close to the low visible energy range, make these nanowires perfect candidates for light emitting devices in optoelectronic applications on the nanoscale.

In table I we also show the magnitude of the band gaps and the binding energy of the intercalated nanowires. All these structures are exothermic, except for 2Cs@Si(30), which is slightly endothermic. Inspection of the binding energies shows three clear trends. First, the Si(30) nanowires are always less stable than the Si(36) due to the unfavorable inter-

action produced by the strong compression in the small Si(30) cages. Second, the alkali intercalations are always less stable than the alkaline-earth, because the radii of the alkali elements are larger than those of the corresponding alkaline-earth and this again increases the possibility of unfavorable interactions. Third, in the alkali atoms the binding energy decreases as the atomic radius increases whereas in the alkaline-earth the trend is just the opposite, with the exception of 2Sr@Si(36). These apparently contradictory behaviors can be again understood in terms of the bigger size of the alkali impurities as compared to the alkaline-earth impurities and the fact that the latter elements donate more charge to the silicon lattice, which stabilizes the structure [20] and increases the bonding with the positive ion.

The band structures of the intercalated nanowires are plotted in Figs. (2) and (3). In the Si(30) structures, all nanowires have a band gap that can be direct at either Γ or X. The only exception to this rule is that corresponding to the lightest element, 2Na@Si(30), where the band gap is slightly indirect. Moving to the bottom of the periodic table, the band gap gradually decreases towards Cs and Ba due to the growing separation between the outer levels of the impurities and the silicon network levels, which decreases the interaction between them. It is interesting to note that in the alkali atoms the magnitude of the gap is reduced by the presence of a low-dispersive state located just above the Fermi level, whereas in the alkaline-earth elements the lowest conduction bands are very dispersive. These features would have important consequences in the transport properties of these systems, giving rise to effects such as negative differential resistance. In the Si(36) structures the situation is rather different. Due to the larger size of the Si(36) cages and the corresponding smaller interaction of the metallic atoms with the silicon structure, the bands of the filled nanowires resemble more closely those of the empty one. For example, in 2K@Si(36), 2Rb@Si(36) and 2Cs@Si(36) the only effect seems to be a rigid downwards shift of the whole silicon band structure. These intercalations give rise to a metallic or semi-metallic behavior, where two bands cross at the X point or open a small band gap. The same behavior is found for all the alkaline-earth intercalations.

The above properties can be understood by separating the effect of the impurities into three parts: a structural deformation and two purely electronic effects associated with charge transfer and hybridization. The structural deformation can be determined by comparing the electronic structure of a relaxed pristine clathrate with the electronic structure of a pristine clathrate in the structural configuration of the intercalated system. We show in Fig. (4) the density of states of the pristine Si(36) nanowire and two typical intercalations corresponding to the most studied intercalated clathrates, sodium and barium [25]. Box (a) corresponds to the pristine and relaxed nanowire, (b) and (d) to the pristine nanowire in the structure of the Na- and Ba-intercalated systems, respectively, and (c) and (e) to the corresponding intercalated nanowires. As can be seen by comparing graphs (a) with (b) or (d), structural modifications are more pronounced in the case of barium en-

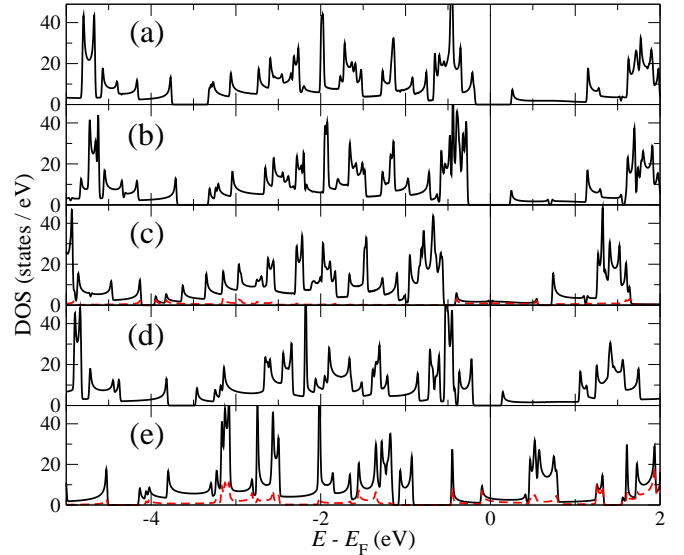


FIG. 4: Projected density of states on the silicon atoms of a pristine Si(36) (a), a Na-deformed pristine Si(36) (b), a 2Na@Si(36) (c), a Ba-deformed pristine Si(36) (d) and a 2Ba@Si(36) (e). The dashed lines in graphs (c) and (e) are the projected densities of states on the Na and Ba atoms, respectively, multiplied by a factor of 3 for clarity.

capsulation due to the larger size of this element. In general, the bigger the atom, the larger the distortion of the lattice. The same behavior is found in the Si(30) nanowires, but due to the smaller endohedral space of the Si_{20} cages and therefore the larger deformation produced by the impurity, the changes are more dramatic. These structural-induced changes in the electronic properties can be understood in terms of the increase or, in some cases, decrease of the distance between neighbor atoms, which reduce or increase the couplings and therefore the bandwidths. The final outcome of the structural deformations is then mainly a modification of the size of the band gaps and widths. In some cases, modification of the bond angles can also move states downwards or upwards depending on whether or not they approach the ideal angles of the sp^3 bonding. This is specially relevant in the Si(30) nanowires.

The effect of charge transfer can be demonstrated by comparing the electronic band structures of the intercalated systems with the pristine ones. Since alkali and alkaline-earth atoms are very electropositive elements, their electronic levels are well above those of silicon and tend to donate the outer one (in the alkali) or two (in the alkaline-earth) electrons to the silicon network. This can be clearly seen in Figs. (2) and (3), where one or two silicon bands move below the Fermi level in the alkali or alkaline-earth intercalations, respectively. Note that since the bands are not spin-split, the number of electrons transferred per unit cell is 2 in the former elements and 4 in the latter, coming from the two atoms in the unit cell.

The hybridization between silicon states and impurity states can be demonstrated by examining the electronic density of states of Fig. (4). As expected, large-diameter elements, such as Ba, interact more strongly with the cage and produce

greater hybridization. This significantly modifies the electronic structure of the intercalated system, compared to that of the isostructural system without the impurity, at the energies where the bands of the endohedral atom are located, as can be easily deduced by looking at the projected density of states on the barium atoms. As a consequence of the presence or absence of hybridization for heavy or light elements, respectively, we conclude that the bond between the bigger impurities and the silicon network in the Si(36), and to a greater extent in the Si(30), is essentially covalent and acquires an increasing ionic character as the size of the atom decreases.

In summary, we have found that the combination of structural deformation, charge transfer and hybridization in alkali or alkaline-earth intercalated silicon clathrate nanowires produces a rich behavior that allows one to tune these systems for technological applications. Their electronic character can range from semiconducting to metallic, which makes them suitable as interconnects for nanocircuits or as other types of electronic elements. Furthermore, the character and width of the band gaps, which in most cases are direct and close to the visible, promise important optoelectronic applications. Finally, the resemblance of these systems to the clathrate bulk phases suggests that superconductivity and novel thermoelectric or elastic properties may be fruitful avenues for future investigations.

We acknowledge financial support from the European Commission and the British EPSRC, DTI, Royal Society, and NWDA. VMGS thanks Jaime Ferrer for useful discussions and the EU network MRTN-CT-2004-504574 for a Marie Curie grant.

- [1] Y. F. Zhang, Y. H. Tang, N. Wang, D. P. Yu, C. S. Lee, I. Bello, and S. T. Lee, *Appl. Phys. Lett.* **72**, 1835 (1998).
- [2] A. M. Morales and C. M. Lieber, *Science* **279**, 208 (1998).
- [3] B. Marsen and K. Sattler, *Phys. Rev. B* **60**, 11593 (1999).
- [4] J. L. Gole, J. D. Stout, W. L. Rauch, and Z. L. Wang, *Appl. Phys. Lett.* **76**, 2346 (2000).
- [5] J. D. Holmes, K. P. Johnston, R. C. Doty and B. A. Korgel,

- Science **287**, 1471 (2000).
- [6] D. D. D. Ma *et al.*, *Science* **299**, 1874 (2003).
- [7] R. P. Wang, G. W. Zhou, Y. L. Liu, S. H. Pan, H. Z. Zhang, D. P. Yu, and Z. Zhang, *Phys. Rev. B* **61**, 16827 (2000).
- [8] M. Durandurdu, *Phys. Stat. Sol B*, **243**, R7 (2006).
- [9] I. Ponomareva, M. Menon, E. Richter, and A. N. Andriotis, *Phys. Rev. B* **74**, 125311 (2006).
- [10] G. Zheng, W. Lu, S. Jin, and C. M. Lieber, *Adv. Mater. (Weinheim. Ger.)* **16**, 1890 (2004).
- [11] M. Menon and E. Richter, *Phys. Rev. Lett.* **83**, 792 (1999).
- [12] B. X. Li, P. L. Cao, R. Q. Zhang, and S. T. Lee, *Phys. Rev. B* **65**, 125305 (2002).
- [13] Y. Zhao and B. I. Yacobson, *Phys. Rev. Lett.* **91**, 035501 (2003).
- [14] X. Zhao, C. M. Wei, L. Yang, and M. Y. Chou, *Phys. Rev. Lett.* **92**, 236805 (2004).
- [15] M. Menon, D. Srivastava, I. Ponomareva, and L. A. Chernozatonskii, *Phys. Rev. B* **70**, 125313 (2004).
- [16] R. Rurrali and N. Lorente, *Phys. Rev. Lett.* **94**, 026805 (2005).
- [17] R. Kagimura, R. W. Nunes, and H. Chacham, *Phys. Rev. Lett.* **95**, 115502 (2005).
- [18] I. Ponomareva, M. Menon, D. Srivastava, and A. N. Andriotis, *Phys. Rev. Lett.* **95**, 265502 (2005).
- [19] A. San-Miguel, P. Kéghélian, X. Blase, P. Mélinon, A. Perez, J. P. Itié, A. Polian, E. Reny, C. Cros, and M. Pouchard, *Phys. Rev. Lett.* **83**, 5290 (1999).
- [20] J. S. Tse, K. Uehara, R. Rousseau, A. Ker, C. I. Ratcliffe, M. A. White, and G. MacKay, *Phys. Rev. Lett.* **85**, 114 (2000).
- [21] J. Gryko, P. F. McMillan, R. F. Marzke, G. K. Ramachandran, D. Patton, S. K. Deb, and O. F. Sankey, *Phys. Rev. B* **62**, R7707 (2000).
- [22] H. Kawaji, H. O. Horie, S. Yamanaka, and M. Ishikawa, *Phys. Rev. Lett.* **74**, 1427 (1995).
- [23] A. San-Miguel and P. Toulemonde, *High Pressure Research* **25**, 159 (2005).
- [24] G. B. Adams, M. O'Keeffe, A. A. Demkov, O. F. Sankey, and Y.-M. Huang, *Phys. Rev. B* **49**, 8048 (1994).
- [25] K. Moriguchi, M. Yonemura, A. Shintani, and S. Yamanaka, *Phys. Rev. B* **61**, 9859 (2000).
- [26] U. Landman, R. N. Barnett, A. G. Scherbakov, and P. Avouris, *Phys. Rev. Lett.* **85**, 1958 (2000).
- [27] J. M. Soler, E. Artacho, J. D. Gale, A. García, J. Junquera, P. Ordejón, and D. Sánchez-Portal, *J. Phys.: Condens. Matter* **14**, 2745 (2002).
- [28] W. Kohn and L. J. Sham, *Phys. Rev.* **140**, A1133 (1965).
- [29] S. F. Boys and F. Bernardi, *Mol. Phys.* **19**, 553 (1970).